

Original Articles

Proteomic analysis of formalin-fixed paraffin-embedded glomeruli suggests depletion of glomerular filtration barrier proteins in two-kidney, one-clip hypertensive rats

Kenneth Finne¹, Heidrun Vethe¹, Trude Skogstrand^{1,2}, Sabine Leh^{1,3}, Tone D. Dahl^{1,2}, Olav Tenstad², Frode S. Berven^{2,4}, Rolf K. Reed^{2,5} and Bjørn Egil Vikse^{1,6,7}

¹Department of Clinical Medicine, University of Bergen, Bergen, Norway, ²Department of Biomedicine, University of Bergen, Bergen, Norway, ³Department of Pathology, Haukeland University Hospital, Bergen, Norway, ⁴The Norwegian Multiple Sclerosis National Competence Centre, Department of Neurology, Haukeland University Hospital, Bergen, Norway, ⁵Centre for Cancer Biomarkers (CCBIO), University of Bergen, Bergen, Norway, ⁶Department of Medicine, Haukeland University Hospital, Bergen, Norway and ⁷Department of Medicine, Haugesund Hospital, Haugesund, Norway

Correspondence and offprint requests to: Kenneth Finne; E-mail: kenneth.finne@k1.uib.no

ABSTRACT

Background. It is well known that hypertension may cause glomerular damage, but the molecular mechanisms involved are still incompletely understood.

Methods. In the present study, we used formalin-fixed paraffin-embedded (FFPE) tissue to investigate changes in the glomerular proteome in the non-clipped kidney of two-kidney one-clip (2K1C) hypertensive rats, with special emphasis on the glomerular filtration barrier. 2K1C hypertension was induced in 6-week-old Wistar Hannover rats ($n = 6$) that were sacrificed 23 weeks later and compared with age-matched sham-operated controls ($n = 6$). Tissue was stored in FFPE tissue blocks and later prepared on tissue slides for laser microdissection. Glomeruli without severe morphological damage were isolated, and the proteomes were analysed using liquid chromatography–tandem mass spectrometry.

Results. 2K1C glomeruli showed reduced abundance of proteins important for slit diaphragm complex, such as nephrin, podocin and nephl. The podocyte foot process had a pattern of reduced abundance of transmembrane proteins but unchanged abundances of the podocyte cytoskeletal proteins synaptopodin and α -actinin-4. Lower abundance of important glomerular basement membrane proteins was seen. Possible glomerular

markers of damage with increased abundance in 2K1C were transgelin, desmin and acyl-coenzyme A thioesterase 1.

Conclusions. Microdissection and tandem mass spectrometry could be used to investigate the proteome of isolated glomeruli from FFPE tissue. Glomerular filtration barrier proteins had reduced abundance in the non-clipped kidney of 2K1C hypertensive rats.

Keywords: 2K1C, FFPE, glomerulus, hypertension, proteomics

INTRODUCTION

Hypertensive nephrosclerosis is a major cause of renal failure worldwide [1], and there is an urgent need for more knowledge about the underlying mechanisms. Glomerular damage occurs early in hypertensive nephrosclerosis [2] and is associated with development of proteinuria and progressive kidney damage [3]. Although it is generally accepted that proteinuria is the result of damage to the glomerular filtration barrier, the detailed biological mechanisms in different glomerular diseases are still not known [4–6].

The two-kidney one-clip (2K1C) hypertensive rat is a model for renovascular hypertension. A silver clip on the renal

artery causes systemic hypertension and hypertensive kidney damage in the non-clipped kidney [7]. Detailed morphological studies have demonstrated podocyte loss as well as podocyte foot process effacement in hypertensive glomerular damage [8–10]. To our knowledge, no studies have previously analysed the isolated glomerular proteome in hypertensive kidney damage, although such a need has been clearly addressed [6].

For decades, formalin-fixed paraffin-embedded (FFPE) tissue blocks have been the standard method of tissue preservation for histopathological examination. Due to its cross-bridging characteristics, tissue fixed in formalin was long considered unsuitable for proteomic analysis but during the last two decades methods to extract proteins from FFPE tissue have been developed [11]. More recently, FFPE protein extraction was combined with tandem mass spectrometry [12, 13], which permitted large scale quantification of proteins in stored biopsies. These methods offer huge opportunities for investigation of the proteomic basis of renal disease due to the large amount of stored FFPE tissue in renal tissue biobanks [14, 15].

The overall objective of the present study was to determine changes in proteins of the glomerular filtration barrier in a model of hypertensive kidney disease. We focused on proteins described as important in a recent review by Patrakka and Tryggvason [5]. Our hypotheses were that microdissected glomerular FFPE tissue could be used for quantitative proteomic analysis and that important glomerular filtration barrier proteins would have lower abundance in 2K1C hypertensive rats compared with sham-operated controls. We used laser microdissection to selectively isolate glomeruli, and reliability of protein extraction was validated using fresh frozen glomeruli samples. The method for quantitative proteomic analysis using small amounts of FFPE glomerular tissue is described.

MATERIALS AND METHODS

Animals and experimental groups

Male Wistar Hannover rats (Taconic, Ry, Denmark) were given free access to tap water and standard rat chow. At 6 weeks of age, the animals were randomly assigned to either 2K1C or control group and hypertension was induced as described previously [16, 17]. Briefly, a silver clip with an internal opening of 0.2 mm was placed on the left renal artery. The controls were sham-operated, but not clipped. All experiments were performed in accordance with, and under the approval of, the Norwegian State Board for Biological Experiments with Living Animals.

Measurements of blood pressure and proteinuria

Blood pressure was measured at 8 weeks after clipping using the tail-cuff method (CODA-6, Kent Scientific, Torrington, CT) as described previously in more detail [17]. Before sacrifice, urine was collected while the rats were kept individually in metabolic cages for 24 h. Urinary protein and creatinine concentrations were analysed in the Laboratories for Clinical Biochemistry at Haukeland University Hospital, Bergen (Roche/Hitachi 912: U/CSF Protein and CREA plus assays).

Sacrifice procedure

At 23 weeks after clipping, six 2K1C and six sham rats were sacrificed under isoflurane anaesthesia as described in more detail previously [18]. The kidneys were flushed with phosphate-buffered saline from the arterial side, removed and weighed. Transversal slices were fixed in 4% buffered formaldehyde, processed by standard procedures and embedded in paraffin.

Tissue preparation and laser capture microdissection

Ten-micrometer FFPE sections were mounted on pre-irradiated polyethylene naphthalate slides (MembraneSlide 1.0 PEN, Carl Zeiss MicroImaging GmbH, Göttingen, Germany), deparaffinized and stained with haematoxylin eosin. Two samples (one from the outer cortex and the other from the juxtamedullary cortex) each with 100 glomerular tuft cross-sections were laser microdissected (PALM MicroBeam, Zeiss) and pressure catapulted into a tube cap (AdhesiveCap 500 clear, Zeiss). Glomeruli with severe morphological damage were excluded as the objective was to investigate early glomerular damage. Total volume of dissected glomerular tissue ranged from 7.8 to 12.5 nL. Dissected FFPE tissue was stored at -20°C .

Isolating fresh frozen glomeruli

Whole glomeruli were isolated using the agarose method described in detail previously [19]. Six sham-operated control rats were sacrificed 13–16 weeks after surgery, and 30 glomeruli were transferred to an eppendorf tube and stored at -80°C until use.

Protein/peptide extraction

Microdissected FFPE glomeruli were suspended in 10 μL lysis solution [0.1 M Tris pH 8, 0.1 M dithiothreitol (DTT), 4% sodium dodecyl sulphate] and heated at 99°C for 60 min. Fresh frozen glomeruli were sonicated, added lysis solution and heated at 95°C for 5 min. The lysate was separated on a NuPAGE Novex 4–12% Bis-Tris at 100 V for 8 min. The gel was stained with Coomassie Brilliant Blue G-250, and one lane was cut into one fraction, which was further cut into cubes of 1 mm^3 . Gel pieces were washed with 50% CH_3CN in 50 mM NH_4HCO_3 , reduced in 10 mM DTT in 100 mM NH_4HCO_3 for 45 min at 56°C and carbamidomethylated with 55 mM iodoacetamide in 100 mM NH_4HCO_3 at room temperature in the dark for 30 min. In-gel tryptic digestion was performed using trypsin porcine (Promega, Fitchburg, WI) at 37°C for 16 h in a 1:20 trypsin:protein ratio. The digested peptides were eluted and desalted using Oasis HLB $\mu\text{Elution}$ plates (Waters, Milford, MA).

Peptide separation and tandem mass spectrometry

The samples, containing an estimated amount of 0.5 μg peptides from FFPE glomeruli and 1 μg from isolated fresh frozen glomeruli (estimated using a bicinchoninic acid assay), were loaded onto a pre-column (Acclaim PepMap 100, 2 $\text{cm} \times 75 \mu\text{m}$ i.d. nanoViper column, packed with 3 μm C18 beads) followed by separation on the analytical column (Dionex

#164570, Acclaim PepMap100 nanoViper column, 75 μm i.d. \times 50 cm, packed with 3 μm C18 beads). Separation by liquid chromatography was performed using an Ultimate 3000 RSLC system (Thermo Scientific, Sunnyvale, CA) connected online to an LTQ-Orbitrap Velos Pro mass spectrometer (Thermo Scientific, Bremen, Germany) equipped with a Nanospray Flex ion source (Thermo Scientific). The peptides were separated using a 180-min LC gradient. The mass spectrometer was operated in data-dependent acquisition mode to automatically switch between full-scan MS and MS/MS acquisition. The seven most intense eluting peptides were sequentially isolated, fragmented and analysed in MS/MS mode.

Label-free quantification

The raw data were analysed with the Progenesis LC-MS software (version 4.0, Nonlinear Dynamics, Newcastle, UK) using default settings. Protein intensity was determined by adding the intensities of all peptides uniquely representing a protein. Relative protein abundance was determined by comparing protein intensities between samples. Features were searched and proteins identified by SearchGUI [20] and PeptideShaker [21] using the UniProtKB *Rattus norvegicus* database (downloaded from UniProt December 2013, 27 316 sequences). Precursor mass tolerance was set at 10 p.p.m. and product mass tolerance at 0.5 Da. Carbamidomethylation of cysteins and oxidation of methionines were set as fixed and variable modifications, respectively. Two missed cleavages were allowed, and false discovery rate was set at 1%.

Histology and immunohistochemistry

Series of 5- μm -thick sections from the non-clipped kidney of 2K1C hypertensive animals and the corresponding kidney from sham-operated control animals were stained for periodic acid-Schiff (PAS), for WT-1 Klon 6F-H2 (M3561 Dako, 1:50) to count podocyte nuclei and for transgelin (SM22- α , ab10135 Abcam PLC, 1:1200 and G1D4 Novus Biologicals, 1:1200), nephrin (Y17-R Novus Biologicals, 1:1200) and synaptopodin (G1D4 Novus Biologicals, 1:400) to validate proteomic findings. Slides were scanned with ScanScope[®] XT (Aperio) at \times 40 and viewed in ImageScope 11. According to the protocol for microdissection, only glomeruli without severe morphological damage

were randomly selected. Identical glomeruli (\geq 10 per animal) in two consecutive series of sections were used for assessment of morphological damage (PAS) and counting of WT-1-positive nuclei per glomerular cross section or glomerular tuft area. Synaptopodin and nephrin staining were quantified by automatic image analysis of 20 glomeruli per kidney using the Aperio positive pixel count algorithm v9.1. If necessary, results were normalized to standard section thickness. Results are expressed as mean number of positive pixels per μm^2 glomerular tuft area.

Electron microscopy

For this investigation, renal tissue from a previous study was used [17]. Small pieces from the renal cortex were fixed in McDowell solution, postfixed in 1% osmium tetroxide and embedded in Epon. Semithin sections were stained with toluidine blue. Blocks with representative changes from two non-clipped kidneys of 2K1C rats and two from sham-operated controls were chosen for ultrastructural investigation. Ultrathin sections were stained with uranyl acetate and lead citrate and studied in a Jeol 100CX electron microscope.

Statistics

Fold change is given for relative quantitation of protein abundance. A protein was considered differentially abundant between 2K1C and controls if identified by at least two unique peptides and had a *t*-test P-value of <0.05 . For other analyses, mean \pm standard deviation (SD) is given and standard two-sided *t*-tests were used for statistical testing and P-values of <0.05 were considered significant unless otherwise noted.

RESULTS

Body weights were similar in the sham-operated control rats and 2K1C rats at start of the experiment, but the 2K1C rats weighed significantly less at time of sacrifice (Table 1). Eight weeks after surgery, the 2K1C rats had higher blood pressure compared with the sham-operated controls ($P = 0.002$). All 2K1C rats had proteinuria and morphological damage characteristic of hypertensive nephropathy at time of sacrifice in contrast to none of the sham rats.

Table 1. Physiological characteristics of 2K1C and sham-operated rats

	Sham ($n = 6$)	2K1C ($n = 6$)	P-value
Weight rat (g)			
0 weeks, surgery	177 \pm 9 ^a	170 \pm 11	0.30
8 weeks	391 \pm 28	365 \pm 23	0.12
23 weeks, sacrifice	495 \pm 32	378 \pm 71	0.01
Kidney weight (g)			
23 weeks, sacrifice	1.42 \pm 0.11	Non-clipped/clipped 1.75 \pm 0.19/1.05 \pm 0.18	0.004/0.003
Blood pressure (mmHg)			
8 weeks			
Systolic	155 \pm 10	206 \pm 28	0.002
Diastolic	108 \pm 9	162 \pm 34	0.005
Proteinuria (g/L)			
23 weeks, sacrifice	0.94 \pm 1.91	4.62 \pm 0.85	0.02

^aThe data are given as mean \pm SD.

Reproducibility and reliability

The reproducibility of the method for extracting proteins from FFPE glomerular tissue was assessed by individually analysing each of the 24 FFPE tissue samples (two samples from each animal, six animals in each group). The number of identified proteins was similar in all the samples, with a mean of 1121 (SD 76, min 960, max 1270). Mean overlap between control samples was 85% (SD 2.2%). The coefficient of variability (CV) was calculated from the protein abundances in samples within the sham and 2K1C group (Supplementary data, Table S1). The median variability was equally low within both groups (21%), indicating a reproducible method work flow [22]. The average variability was, however, higher within the 2K1C animals when compared with sham rats (28 versus 23%).

The chemical modifications produced by the fixation process [23] may influence protein extraction from FFPE tissue. We investigated differences in the identified proteins from FFPE tissue and fresh frozen tissue by comparing the overlap of identified proteins between 12 FFPE glomerular samples from controls (six animals, two samples from each) with the same number of fresh frozen glomeruli samples. A total of 1303 proteins were identified from the FFPE sham glomeruli and 1781 from the fresh frozen sham glomeruli. Of the 1303 proteins from FFPE glomeruli, 83% overlapped with proteins from fresh frozen glomeruli, presented as a Venn diagram in Figure 1.

Changes in glomerular proteome in 2K1C versus sham

Combining the data from all 24 FFPE tissue samples using label-free quantification, 8451 unique peptides (9585 in total) were identified. The identified peptides correspond to a total of 1417 proteins (Supplementary data, Table S2), of which 1066 proteins were identified with two or more unique peptides, and used for protein quantification (Supplementary data, Table S1). The analysis demonstrated that 185 proteins

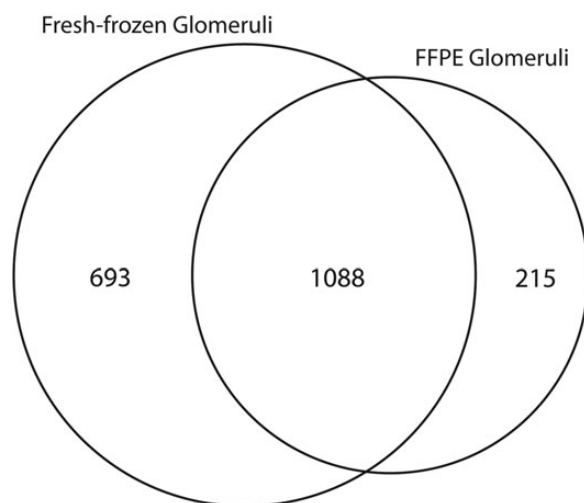


FIGURE 1: Number of identified proteins from FFPE and fresh frozen glomeruli from sham-operated controls. A total of 1781 proteins were identified in fresh frozen samples, compared with 1303 in FFPE samples. In total, 1088 proteins overlapped, corresponding to 83% of the total identifications from FFPE glomeruli.

were more abundant in 2K1C glomeruli compared with controls and 206 proteins were less abundant.

We investigated changes in the glomerular filtration barrier proteome following hypertensive injury by comparing relative abundances (2K1C/sham) of proteins known to play a role in the slit diaphragm complex, the podocyte foot process and the glomerular basement membrane (GBM). We used Figure 2 (adapted from Patrakka and Tryggvason [5] and printed with permission in this paper) as a basis for relevant proteins.

Podocyte foot process and the slit diaphragm complex. Of the 19 podocyte foot process proteins (Figure 2), we were able to quantify 15 from the glomerular samples (Table 2). Podocyte foot process cytoskeletal proteins, such as β -actin, α -actinin-4 and synaptopodin [24, 25], were unchanged in 2K1C compared with controls. In addition, no change was seen for actin-related proteins (actin-related protein 3, F-actin-capping protein subunit beta, fascin, tropomyosin alpha-1 chain) (data not shown).

Of the 18 slit diaphragm complex proteins in Figure 2, we were able to quantify 12 from the glomerular samples, 11 of which showed lower abundance in 2K1C compared with controls (Table 3). Among these were several well characterized slit diaphragm proteins such as nephrin, neph1, podocin and ZO-1. However, the most significantly reduced proteins were the less studied proteins Magi2 and Pard3b. Additionally, roundabout homolog 2 (robo2), a protein recently found to interact with nephrin in the slit diaphragm [26], showed reduced abundance similar to nephrin.

The glomerular basement membrane. Most major proteins of the GBM, which have previously been described in the literature [27], were identified in the glomerular tissue. Of the GBM proteins, collagen IV α 3 and α 5 chains, laminin chains α 5, β 2 and γ 1, nidogen-1 and agrin displayed significantly reduced abundance in 2K1C as compared with sham (Table 4).

Potential glomerular damage markers. Table 5 presents a list of potential glomerular damage markers in hypertensive glomerular injury in the present study. The list contains all proteins that were at least 30% more abundant in 2K1C rats as compared with sham-operated controls (with a $P < 0.01$). Only proteins that were not abundant in plasma (< 100 peptide-spectrum matches in [28]), and that overlapped with already mapped glomerulus proteins [29] were included. In total, 23 proteins fulfilled the criteria and the proteins with the highest relative change in 2K1C were transgelin, acyl-coenzyme A thioesterase 1 and desmin (Table 5).

Morphological changes in 2K1C versus sham

The non-clipped kidney of 2K1C rats showed significant morphological damage when compared with corresponding kidneys in sham-operated rats (Figure 3). Glomerular morphology in 2K1C varied from normal-to-mild morphological damage (mesangial widening, absorption droplets in podocytes) to more severe morphological damages (adherences, segmental sclerosis, as well as pronounced ischaemic changes and thrombotic microangiopathy in some rats). Hypertensive vasculopathy was prominent, and acute and chronic tubulointerstitial

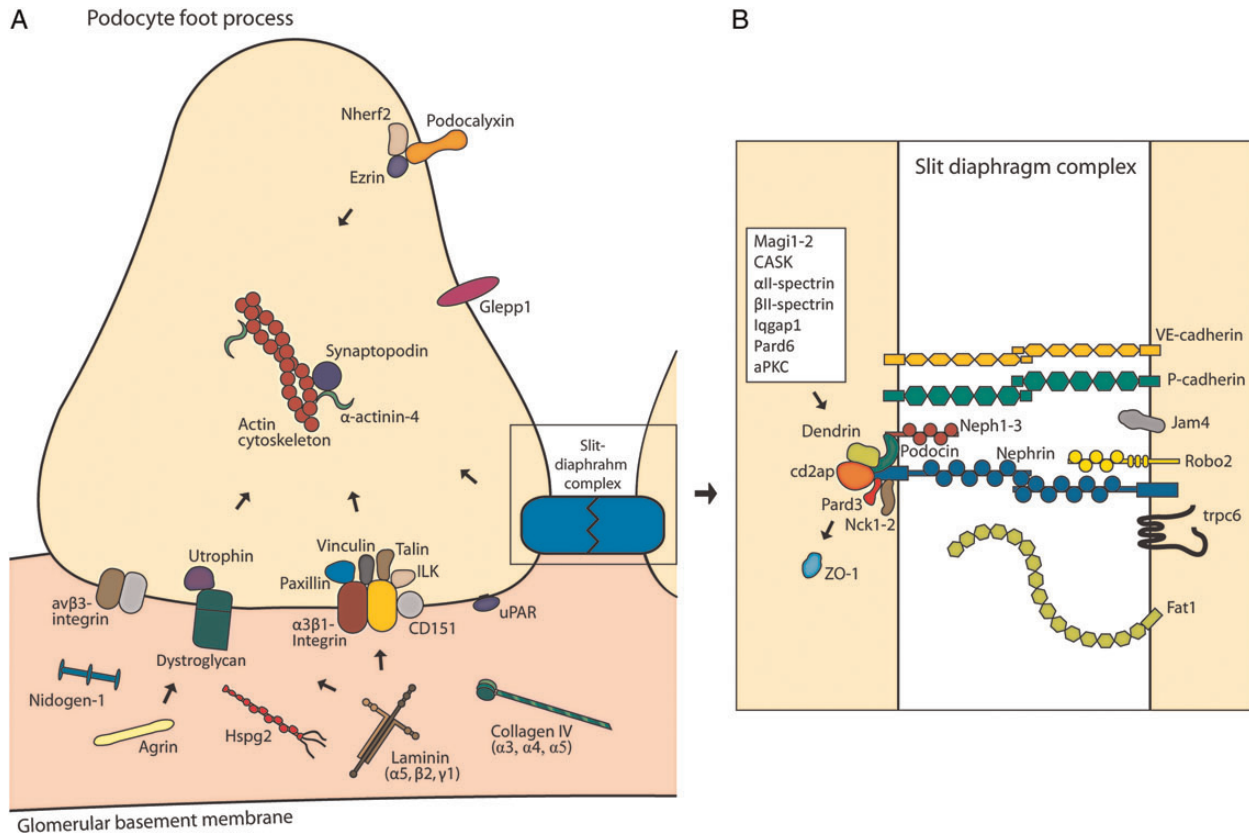


FIGURE 2: Important proteins of the glomerular filtration barrier. (A) Proteins of the podocyte foot process and GBM. (B) Proteins of the slit diaphragm complex. Modified from and printed with permission from Patrakka and Tryggvason [5].

Table 2. Abundance of podocyte foot process proteins in 2K1C as compared with sham-operated rats

Protein	Gene	2K1C versus sham	
		Relative abundance	P-value
Cytoskeletal proteins			
Synaptopodin	Synpo	0.86	0.16
α -Actinin-4	Actn4	0.92	0.23
Actin, cytoplasmic 1	Actb	1.04	0.74
Actin, cytoplasmic 2	Actc	1.24	0.003
Transmembrane proteins			
Ptpro (glepp1)	Glepp1	0.78	0.002
$\alpha 3$ -Integrin	Itga3	0.80	<0.001
$\beta 1$ -Integrin	Itgb1	0.81	0.002
Podocalyxin	Podxl	0.89	0.18
Dystroglycan	Dag1	0.91	0.26
αv -Integrin	Itgav	1.05	0.63
$\beta 3$ -Integrin	Itgb3	N/A	–
CD151 antigen	Cd151	N/A	–
Urokinase plasminogen activator surface receptor	Plaur	N/A	–
Adaptor proteins			
Talin	Tln1	0.85	0.01
Na(+)/H(+) exchange regulatory cofactor NHE-RF2	Nherf2	0.87	0.15
Ezrin	Ezr	0.89	0.06
Utrophin	Utrn	0.89	0.11
Integrin-linked protein kinase	Ilk	0.93	0.29
Vinculin	Vcl	1.01	0.86
Paxillin	Pxn	N/A	–

damage was present. For the proteomic analyses in the present study, we did not microdissect glomeruli with severe morphological damage.

A representative sample of 2K1C glomeruli eligible for microdissection was compared with sham rats; glomeruli from 2K1C rats had lower mean glomerular tuft area, a non-significant trend towards a lower number of WT-1-positive podocyte nuclei per glomerular cross section and a significantly lower number per glomerular area (Table 6). As a sign of a defect filtration barrier, podocytes from 2K1C glomeruli often contained absorption droplets. Less than 5% of glomeruli eligible for microdissection showed ischaemia, adhesences, endothelial swelling, segmental sclerosis or pseudocysts. Qualitative electron microscopy of representative glomeruli from 2K1C non-clipped kidneys showed enlarged podocytes with electron dense membrane-bound absorption droplets and mild segmental foot process effacement, basement membrane changes were not observed (Figure 3).

To validate proteomic findings, immunohistochemistry for nephrin, synaptopodin and transgelin was performed (Figure 4). As expected from the proteomic findings, synaptopodin showed a similar amount of positivity in 2K1C and sham glomeruli. Nephrin showed a tendency to lower expression in 2K1C glomeruli with a 2K1C/sham ratio of 0.9 (not significant, $P = 0.15$). Nephrin staining correlated significantly with nephrin proteomic intensity ($r^2 = 0.44$, $P = 0.02$, Supplementary data, Figure S1). Proteomic results indicated transgelin as a potential glomerular damage marker. 2K1C glomeruli showed *de novo* staining in

Table 3. Abundance of slit diaphragm complex proteins in 2K1C as compared with sham rats

Protein	Gene	2K1C versus sham	
		Relative abundance	P-value
Membrane-associated guanylate kinase, WW and PDZ domain-containing protein 2	Magi2	0.64	<0.001
Dendrin	Dnd	0.65	<0.001
Protein Pard3b	Pard3b	0.65	<0.001
Kin of IRRE-like protein 1	Neph1	0.68	<0.001
Roundabout homolog 2	Robo2	0.69	<0.001
Par-6 (partitioning defective 6) homolog beta	Pard6	0.69	<0.01
Nephrin	Nphs1	0.72	<0.001
Podocin	Nphs2	0.77	<0.01
Tight junction protein ZO-1	Tjp1	0.77	<0.001
Spectrin beta chain, non-erythrocytic 1 (β -II spectrin)	Sptbn1	0.80	<0.001
Spectrin alpha chain, non-erythrocytic 1 (α -II spectrin)	Sptan1	0.82	<0.001
Protein CD2AP	Cd2ap	0.87	0.03
IQ motif containing GTPase activating protein 1	Iqgap1	0.93	0.21
Peripheral plasma membrane protein CASK	Cask	N/A	–
NCK1-2	Nck1-2	N/A	–
P-cadherin	Cdh3	N/A	–
VE-cadherin	Cdh5	N/A	–
Short transient receptor potential channel 6	Trpc6	N/A	–
Junctional adhesion molecule 4	Jam4	N/A	–
Protein Fat1	Fat1	N/A	–

Table 4. Abundance of GBM proteins in 2K1C as compared with sham-operated rats

Protein	Gene	2K1C versus sham	
		Relative abundance	P-value
Agrin	Agrn	0.61	<0.0001
Collagen alpha 3 Type IV	Col4a3	0.69	0.03
Collagen alpha 4 Type IV	Col4a4	N/A	–
Collagen alpha 5 Type IV	Col4a5	0.69	0.03
Laminin alpha 5	Lama5	0.70	0.007
Laminin beta 2	Lamb2	0.71	0.01
Laminin gamma 1	Lamc1	0.70	0.01
Nidogen-1	Nid	0.72	0.01
Protein Hspg2	Hspg2	0.84	0.20

some podocytes as well as stronger staining in the parietal epithelium and the glomerular vascular pole (Figure 4).

DISCUSSION

In the present study, we have investigated quantitative changes in the glomerular proteome in hypertensive nephropathy. Glomeruli without severe morphological damage were micro-dissected from FFPE renal tissue, and small amounts of tissue were used for quantitative proteomic analysis. Protein

Table 5. List of potential glomerular damage markers in 2K1C hypertension

Protein	Gene	2K1C versus sham	
		Relative abundance	P-value
Transgelin	Tagln	3.41	<0.01
Acyl-coenzyme A thioesterase 1	Acot1	3.19	<0.01
Desmin	Des	2.43	<0.0001
Acid ceramidase	Asah1	2.16	<0.0001
Alpha-crystallin B chain	Cryab	1.74	<0.001
Ficolin (collagen/fibrinogen domain containing) 1	Fcn1	1.86	<0.01
Ferritin light chain 1	Ftl1	1.86	<0.01
Glutamyl aminopeptidase	Enpep	1.62	<0.0001
NADH-cytochrome b5 reductase 3	Cyb5r3	1.51	<0.0001
Major vault protein	Mvp	1.44	<0.01
NADH dehydrogenase [ubiquinone] flavoprotein 2, mitochondrial	Ndufv2	1.43	<0.001
Heat shock 27 kDa protein 1	Hspb1	1.43	<0.01
Lactadherin	Mfge8	1.40	<0.01
60S ribosomal protein L12	Rpl12	1.39	<0.01
Atlastin-3	Atl3	1.38	<0.001
Coronin-1C	Coro1c	1.38	<0.0001
40S ribosomal protein S10	Rps10	1.38	<0.001
Protein Serpinb6	Serpinb6	1.37	<0.0001
Pyruvate kinase PKM	PKM	1.37	<0.0001
Glucose-6-phosphate 1-dehydrogenase	G6pd	1.36	<0.01
Nestin	Nes	1.32	<0.01
60S acidic ribosomal protein P0	Rplp0	1.31	<0.001
NADH dehydrogenase (ubiquinone) flavoprotein 1	Ndufv1	1.30	<0.001

extraction was shown to be reproducible and reliable. We demonstrated that proteins important for the glomerular filtration barrier were 20–40% less abundant in glomeruli from 2K1C rats when compared with sham rats. Proteins important for the podocyte cytoskeleton were not changed. Morphologically, we demonstrated glomerular hypertrophy in 2K1C and a significantly lower number of podocytes per glomerular tuft area. Transgelin, desmin and acyl-coenzyme A thioesterase 1 were identified as possible markers of hypertension-induced glomerular damage.

The podocyte has been subject to detailed study during the last decades [30], and mapping of the intracellular processes within the podocyte is emerging [31]. In the present study, we used a label-free proteomics approach to quantitatively compare glomerular proteins from 2K1C rats with hypertensive kidney damage to sham-operated controls. We were able to quantify over a 1000 proteins and in order to study proteins important for the glomerular filtration barrier; we chose to focus on proteins described in a recent review by Patrakka and Tryggvason [5]. The slit diaphragm proteins, nephrin and podocin, have previously been shown to be associated with podocyte foot process effacement and are reduced in hypertensive nephrosclerosis [8, 10]. Gene expression analyses have also shown downregulation of nephrin, podocin, magi2 and ZO-1 in other glomerular diseases, like focal segmental glomerulosclerosis [32, 33]. Our results support these findings,

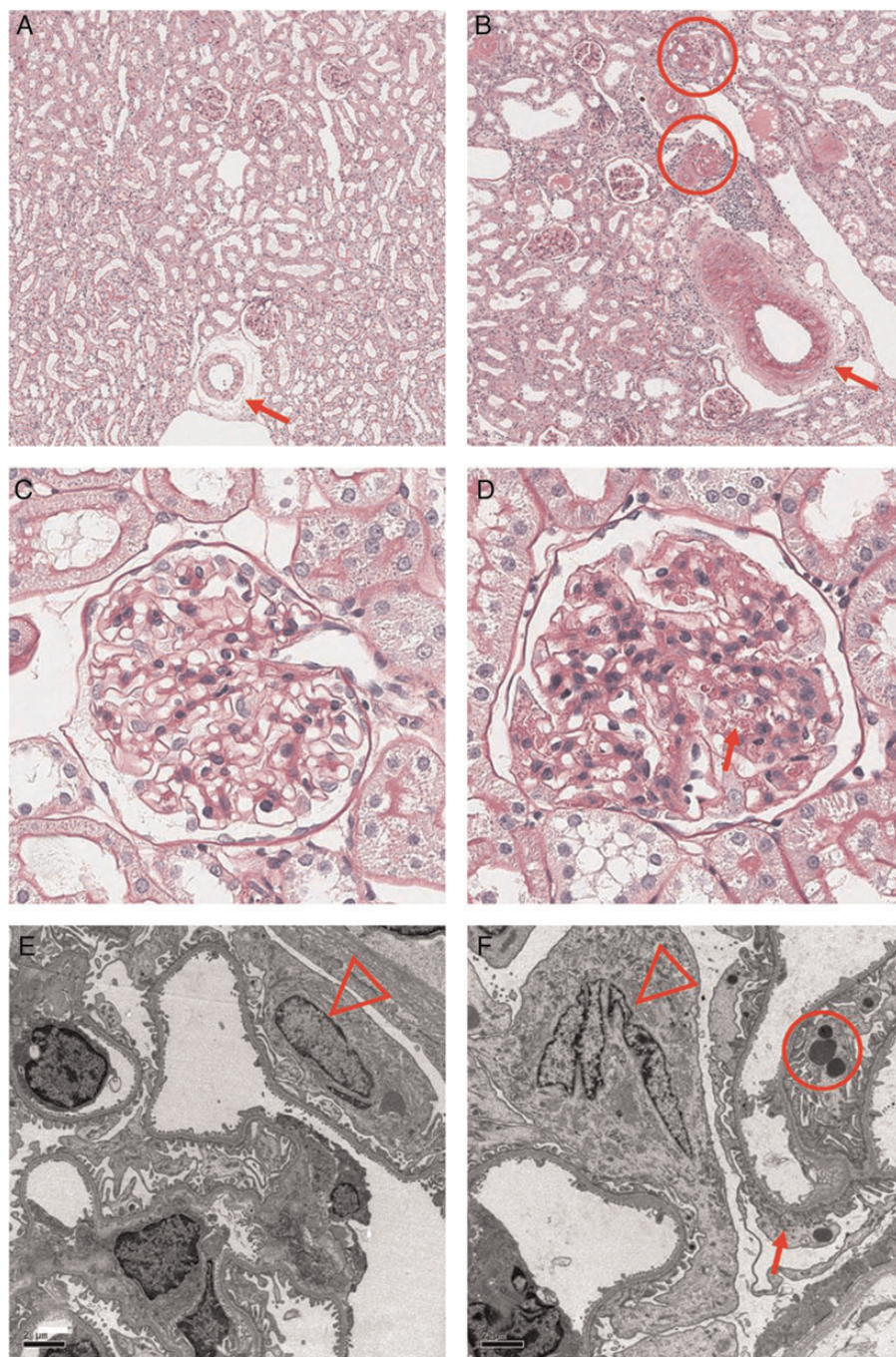


FIGURE 3: Histological (A–D) and ultrastructural (E and F) characteristics of the unclipped kidney in 2K1C (B, D and F) versus sham-operated control rats (A, C and E). (A and B) An overview image from the juxtamedullary cortex with arcuate arteries (arrows, notice pronounced wall hypertrophy in B). Encircled glomeruli in (B) show severe morphologic changes and are not eligible for microdissection. (D) shows a typical glomerulus, chosen for microdissection, with minor mesangial changes and absorption droplets in podocytes (arrow). Ultrastructurally these glomeruli (F) show enlarged podocytes compared with sham podocytes (E, arrowheads). In addition, the glomerulus in (F) shows electron dense absorption droplets (circle) indicating proteinuria and segmental foot process effacement (arrow).

but show that also the other slit diaphragm proteins are less abundant in 2K1C. Several podocyte transmembrane proteins identified in the present study show reduced abundance in 2K1C, including $\alpha\beta1$ -integrin, the major podocyte integrin involved in GBM binding [5] and *glepp1* that is important for maintaining podocyte structure and function [34, 35]. This is supported by previous studies that showed decreased

abundance of $\alpha\beta1$ -integrin in podocytes subjected to mechanical stress *in vitro* [36] as well as in diabetic nephropathy [37], suggesting a possible factor in podocyte detachment. Downregulation of *glepp1* is previously reported as an early marker for podocyte injury. Interestingly, regulation of *glepp1* precedes change in podocalyxin expression [34], which is consistent with the results in the present study. Several studies on

Table 6. Morphological characteristics of glomeruli eligible for proteomic analysis

	Sham (<i>n</i> = 6)	2K1C (<i>n</i> = 6)	P-value
Glomerular morphology			
Mean glomerular area (μm^2)	8640 \pm 1080	10 600 \pm 1770	0.004
Number of podocyte nuclei ^a per glomerular cross section	12.6 \pm 2.1	10.9 \pm 2.2	0.07
Number of podocyte nuclei ^a per 1000 μm^2 glomerular area	1.46 \pm 0.12	1.07 \pm 0.33	0.001
Glomerular lesions (% positive glomeruli)			
Absorption droplets	0	21.4 \pm 10.8	0.002
Ischaemia	0	0.8 \pm 1.9	0.18
Adherences	0	4.8 \pm 5.7	0.05
Endothelial swelling	0	4.8 \pm 6.5	0.09
Segmental sclerosis	0	0.8 \pm 2.0	0.18
Pseudocysts	0	1.9 \pm 3.0	0.09

^aCounted as WT-1-positive nuclei per glomerular cross section.

hypertensive nephrosclerosis have shown reduced abundance of the actin-associated proteins α -actinin-4 and synaptopodin [10, 38, 39]. However, common for these studies is a prominent degree of glomerulosclerosis, a feature that in mutational studies has been shown to be mediated by dysfunction of these proteins [40, 41]. In the present study, only glomeruli without severe morphological damage were microdissected and we believe that this explains the apparent discrepancy between the present and previous studies. The present study also demonstrated reduced abundance of the proteins from the GBM in the glomeruli from hypertensive rats. Qualitative electron microscopy in the present study and a previous study on hypertensive nephrosclerosis [42] did not show significant thinning of the GBM, and our proteomic finding does not seem to have a clear morphological explanation. To our knowledge, no studies have investigated the proteome of the GBM in hypertensive nephrosclerosis and our novel findings will need confirmation and further investigation in future studies.

To investigate the reliability of extracted proteins from FFPE glomeruli for use in proteomic analyses, we compared the identified proteins from FFPE glomeruli with the identified proteins from isolated fresh frozen glomeruli. As more tissue was used when analysing fresh frozen glomeruli (1 μg) as compared with when analysing FFPE glomeruli (0.5 μg), the 40% higher number of identified proteins in fresh frozen glomeruli in the present study could be expected, although it is likely that the number of identifications using fresh frozen glomeruli would be higher also with equal tissue amounts. Importantly, 83% of proteins from FFPE samples could be identified also in the fresh frozen samples. This is only slightly lower than the overlap between two separate samples containing glomeruli from FFPE tissue (85% overlap) or fresh frozen tissue (86%, data not shown). In general, the quality of protein identifications was at least similar, and possibly even better than other studies that compare fresh frozen and FFPE prepared material from other tissues, using gel-based methods [43, 44]. A few previous studies have analysed the glomerular proteome in fresh frozen [45] and

FFPE tissue [46, 47]; however, these identified significantly fewer proteins than the present study. This is noteworthy considering the low amount of glomerular FFPE tissue used in our study (10 nL); we attribute a large part of this to the use of state-of-the-art LC-MS/MS technology used in our study. Based on the high degree of overlap with isolated fresh frozen samples, high number of identified proteins per sample, low variation in numbers of identified proteins between samples, low CV within groups, high consistency between findings for relative quantity for different proteins from the same compartment, as well as similar findings in immunohistochemistry validation, we conclude that our method is well suited for further analyses of the glomerular proteome.

As the glomerulus consists of several cell types, podocytes, mesangial cells and endothelial cells, it is possible that altered balance between these cell types could account for some of the proteome changes described in the present study. To minimize such potential differences, we chose only to microdissect glomeruli without severe morphological damage. Glomerular hypertrophy is a common feature of hypertensive kidney disease [42, 48] and was also observed in glomeruli included in this study. The expanding tuft surface area requires the podocyte to stretch, a potential pathological response that is followed by foot process effacement, podocyte detachment and focal segmental glomerulosclerosis [42, 49]. The unchanged abundance of the podocyte-specific cytoskeletal protein synaptopodin, validated by immunohistochemistry, indicates that the ratio between podocyte cell volume and total cell volume did not change much. Both the glomerular tuft area and the podocytes were larger in 2K1C as compared with sham. As the podocyte cell count was lower per glomerular area in hypertensive compared with normotensive rats, and electron microscopy did not show denudation of glomerular capillaries, this indicates that the podocytes had undergone hypertrophy. Electron microscopy also showed mild foot process fusion in 2K1C, a trait that is expected to result in a lower foot process surface area. Although uncertain, the reduced abundance of proteins from the slit diaphragm and other transmembrane proteins of the foot processes may be partly explained by the observed morphological changes. Further studies will need to investigate whether primary molecular changes with loss of slit diaphragm proteins can play a pathophysiological role.

We also examined proteins identified in the present study that could be potential damage markers for glomerular injury with focus on proteins already mapped to the glomerulus [29] and with a relative increase in abundance >30% in 2K1C. Proteins known to be abundant in plasma [28] were excluded. The three proteins with the highest relative abundance in 2K1C compared with controls were desmin, acyl-coenzyme A thioesterase 1 and transgelin. Desmin is an intermediate filament protein that has also previously been found to be up-regulated in podocytes of the non-clipped kidney 2K1C hypertensive rats [50] and is suggested as a marker for glomerular injury in puromycin aminonucleoside nephrosis [51] and diabetic nephropathy [52] in rat models. Transgelin is upregulated in podocytes of several nephropathies [53, 54] and has been reported as markers for repopulating mesangial cells in response to damage [55]. The former was also suggested by our

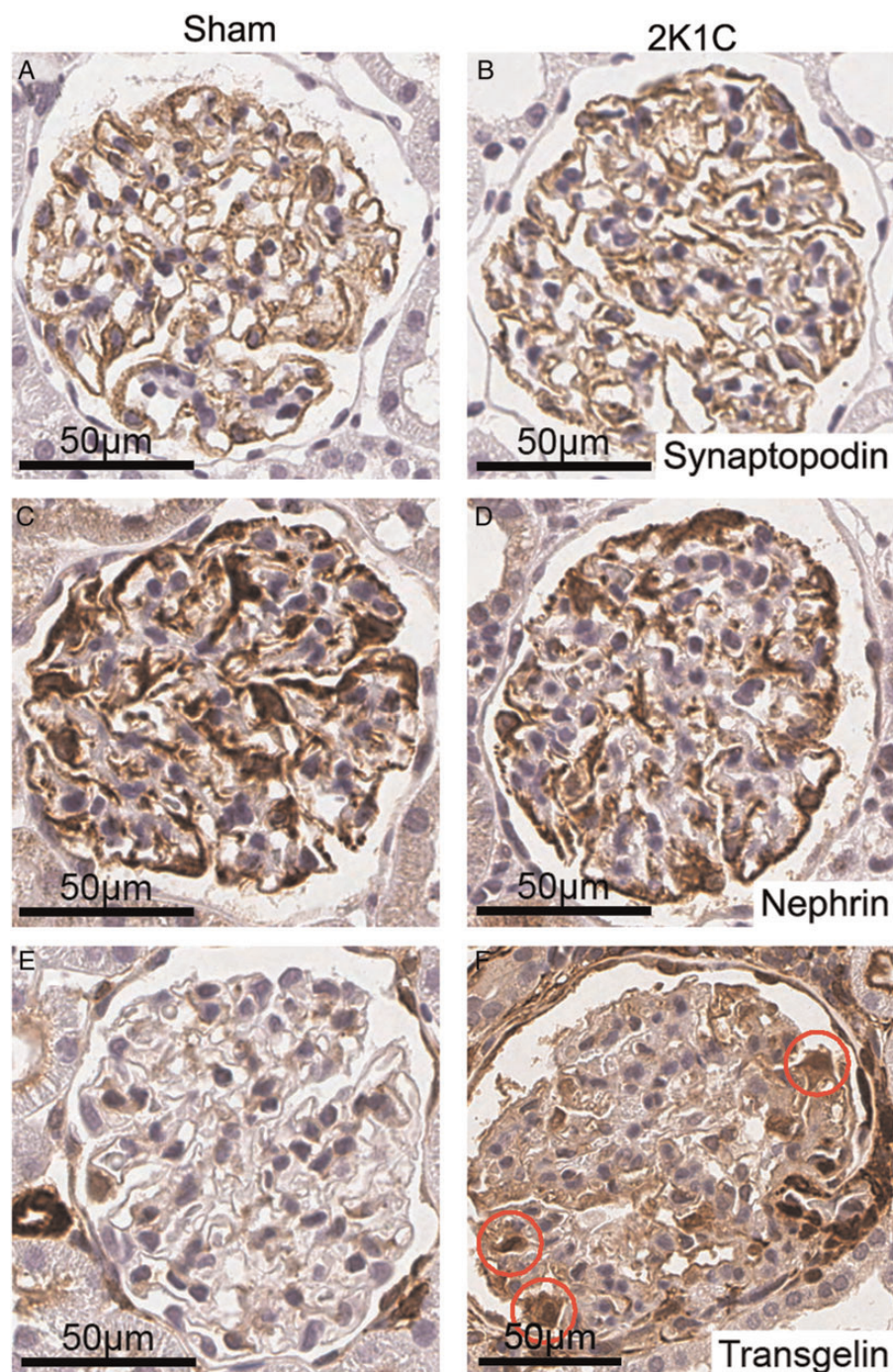


FIGURE 4: Immunohistochemistry for synaptopodin, nephrin and transgelin in glomeruli from 2K1C and sham. Representative micrographs are presented. (A and B) Synaptopodin shows a linear staining along the capillary wall and is identical in sham and 2K1C. (C and D) Nephrin is positive in podocytes with a linear staining along the capillary wall. Positivity is slightly decreased in 2K1C as compared with sham, in statistical analyses this did not reach significance ($P = 0.15$). (E and F) Transgelin is negative in sham, whereas some podocytes (red circles) are positive in 2K1C. There is also increased positivity in the parietal epithelium and the glomerular vascular pole in 2K1C.

immunohistochemistry findings. Acyl-coenzyme A thioesterase 1 is involved in intracellular lipid metabolism [56], but its role in disease has not been studied.

In conclusion, the present study has demonstrated a reliable and reproducible method for extracting proteins from small amounts of FFPE glomerular tissue for quantitative proteomic analyses. In 2K1C hypertensive rats, we demonstrated reduced

abundance of podocyte proteins from the slit diaphragm complex and proteins important for the interaction with the glomerulus basal membrane. Furthermore, potential damage markers have been presented, with desmin, transgelin and acyl-coenzyme A thioesterase 1 being the most interesting for future research. Future studies of the glomerular proteome at different stages of hypertensive nephrosclerosis will be

important for a more detailed characterization of the underlying mechanisms.

SUPPLEMENTARY DATA

Supplementary data are available online at <http://ndt.oxfordjournals.org>.

ACKNOWLEDGEMENTS

Microdissection of glomerular tissue was performed using equipment from the Molecular Imaging Center (Fuge, Norwegian Research Council), University of Bergen. Thanks to Edith Fick, Department of Clinical Medicine, for preparing tissue sections. The proteomic analyses were performed at the Proteomic Unit at the University of Bergen (PROBE). Special thanks to Olav Mjaavatten for technical assistance. Thanks to Dagny Ann Sandnes, Department of Clinical Medicine, University of Bergen, for immunohistochemistry. We are also indebted to Ann-Kristin Straus Dahl, Hilde Fløystad, Bendik Nordanger, Nina Holmelid and Brynhild Haugen, Department of Pathology, Haukeland University Hospital, for skillful technical assistance.

FUNDING

The study was supported by research grants from the Western Norway Regional Health Authority. Vikse BE held from 2012 to 2014 a part-time professorial position at the University of Bergen that was partly financed by Amgen Inc.

CONFLICT OF INTEREST STATEMENT

None declared.

REFERENCES

1. Luke RG. Hypertensive nephrosclerosis: pathogenesis and prevalence. Essential hypertension is an important cause of end-stage renal disease. *Nephrol Dial Transplant* 1999; 14: 2271–2278
2. Remuzzi G, Bertani T. Pathophysiology of progressive nephropathies. *N Engl J Med* 1998; 339: 1448–1456
3. Ruggenti P, Cravedi P, Remuzzi G. Mechanisms and treatment of CKD. *J Am Soc Nephrol* 2012; 23: 1917–1928
4. Haraldsson B, Nystrom J, Deen WM. Properties of the glomerular barrier and mechanisms of proteinuria. *Physiol Rev* 2008; 88: 451–487
5. Patrakka J, Tryggvason K. Molecular make-up of the glomerular filtration barrier. *Biochem Biophys Res Commun* 2010; 396: 164–169
6. Tryggvason SH, Guo J, Nukui M *et al*. A meta-analysis of expression signatures in glomerular disease. *Kidney Int* 2013; 84: 591–599
7. Navar LG, Zou L, Von Thun A *et al*. Unraveling the mystery of Goldblatt hypertension. *News Physiol Sci* 1998; 13: 170–176
8. Nagase M, Shibata S, Yoshida S *et al*. Podocyte injury underlies the glomerulopathy of Dahl salt-hypertensive rats and is reversed by aldosterone blocker. *Hypertension* 2006; 47: 1084–1093
9. Kriz W, Shirato I, Nagata M *et al*. The podocyte's response to stress: the enigma of foot process effacement. *Am J Physiol Renal Physiol* 2013; 304: F333–F347
10. Wang G, Lai FM, Kwan BC *et al*. Podocyte loss in human hypertensive nephrosclerosis. *Am J Hypertens* 2009; 22: 300–306
11. Ikeda K, Monden T, Kanoh T *et al*. Extraction and analysis of diagnostically useful proteins from formalin-fixed, paraffin-embedded tissue sections. *J Histochem Cytochem* 1998; 46: 397–403
12. Crockett DK, Lin Z, Vaughn CP *et al*. Identification of proteins from formalin-fixed paraffin-embedded cells by LC-MS/MS. *Lab Invest* 2005; 85: 1405–1415
13. Palmer-Toy DE, Krastins B, Sarracino DA *et al*. Efficient method for the proteomic analysis of fixed and embedded tissues. *J Proteome Res* 2005; 4: 2404–2411
14. Craven RA, Cairns DA, Zougman A *et al*. Proteomic analysis of formalin-fixed paraffin-embedded renal tissue samples by label-free MS: assessment of overall technical variability and the impact of block age. *Proteomics Clin Appl* 2013; 7: 273–282
15. Sedor JR. Tissue proteomics: a new investigative tool for renal biopsy analysis. *Kidney Int* 2009; 75: 876–879
16. Helle F, Vagnes OB, Iversen BM. Angiotensin II-induced calcium signaling in the afferent arteriole from rats with two-kidney, one-clip hypertension. *Am J Physiol Renal Physiol* 2006; 291: F140–F147
17. Skogstrand T, Leh S, Paliege A *et al*. Arterial damage precedes the development of interstitial damage in the nonclipped kidney of two-kidney, one-clip hypertensive rats. *J Hypertens* 2013; 31: 152–159
18. Hultstrom M, Leh S, Skogstrand T *et al*. Upregulation of tissue inhibitor of metalloproteinases-1 (TIMP-1) and procollagen-N-peptidase in hypertension-induced renal damage. *Nephrol Dial Transplant* 2008; 23: 896–903
19. Hook U, Svalander CT. Agarose method for the preparation of isolated glomeruli from human renal biopsies. *APMIS* 1991; 99: 844–848
20. Vaudel M, Barsnes H, Berven FS *et al*. SearchGUI: an open-source graphical user interface for simultaneous OMSSA and X!Tandem searches. *Proteomics* 2011; 11: 996–999
21. Barsnes H, Vaudel M, Colaert N *et al*. Compomics-utilities: an open-source Java library for computational proteomics. *BMC Bioinformatics* 2011; 12: 70
22. Nagaraj N, Mann M. Quantitative analysis of the intra- and inter-individual variability of the normal urinary proteome. *J Proteome Res* 2011; 10: 637–645
23. Metz B, Kersten GF, Hoogerhout P *et al*. Identification of formaldehyde-induced modifications in proteins: reactions with model peptides. *J Biol Chem* 2004; 279: 6235–6243
24. Bariety J, Bruneval P, Hill G *et al*. Posttransplantation relapse of FSGS is characterized by glomerular epithelial cell transdifferentiation. *J Am Soc Nephrol* 2001; 12: 261–274
25. Ichimura K, Kurihara H, Sakai T. Actin filament organization of foot processes in rat podocytes. *J Histochem Cytochem* 2003; 51: 1589–1600
26. Fan X, Li Q, Pisarek-Horowitz A *et al*. Inhibitory effects of Robo2 on nephrin: a crosstalk between positive and negative signals regulating podocyte structure. *Cell Rep* 2012; 2: 52–61
27. Miner JH. Renal basement membrane components. *Kidney Int* 1999; 56: 2016–2024
28. Farrah T, Deutsch EW, Omenn GS *et al*. A high-confidence human plasma proteome reference set with estimated concentrations in PeptideAtlas. *Mol Cell Proteomics* 2011; 10: M110.006353
29. Cui Z, Yoshida Y, Xu B *et al*. Profiling and annotation of human kidney glomerulus proteome. *Proteome Sci* 2013; 11: 13
30. Pavenstadt H, Kriz W, Kretzler M. Cell biology of the glomerular podocyte. *Physiol Rev* 2003; 83: 253–307
31. Warsow G, Endlich N, Schordan E *et al*. PodNet, a protein-protein interaction network of the podocyte. *Kidney Int* 2013; 84: 104–115
32. Matsusaka T, Sandgren E, Shintani A *et al*. Podocyte injury damages other podocytes. *J Am Soc Nephrol* 2011; 22: 1275–1285
33. Hodgkin JB, Borczuk AC, Nasr SH *et al*. A molecular profile of focal segmental glomerulosclerosis from formalin-fixed, paraffin-embedded tissue. *Am J Pathol* 2010; 177: 1674–1686
34. Kim YH, Goyal M, Wharram B *et al*. GLEPP1 receptor tyrosine phosphatase (Ptpro) in rat PAN nephrosis. A marker of acute podocyte injury. *Nephron* 2002; 90: 471–476

35. Thomas PE, Wharram BL, Goyal M *et al.* GLEPP1, a renal glomerular epithelial cell (podocyte) membrane protein-tyrosine phosphatase. Identification, molecular cloning, and characterization in rabbit. *J Biol Chem* 1994; 269: 19953–19962
36. Dessapt C, Baradez MO, Hayward A *et al.* Mechanical forces and TGF beta 1 reduce podocyte adhesion through alpha 3 beta 1 integrin downregulation. *Nephrol Dial Transplant* 2009; 24: 2645–2655
37. Chen HC, Chen CA, Guh JY *et al.* Altering expression of alpha 3 beta 1 integrin on podocytes of human and rats with diabetes. *Life Sci* 2000; 67: 2345–2353
38. Hayata M, Kakizoe Y, Uchimura K *et al.* Effect of a serine protease inhibitor on the progression of chronic renal failure. *Am J Physiol Renal Physiol* 2012; 303: F1126–F1135
39. Yasuno K, Araki S, Sakashita H *et al.* Development of podocyte injuries in Osborne-Mendel rats is accompanied by reduced expression of podocyte proteins. *J Comp Pathol* 2013; 149: 280–290
40. Kaplan JM, Kim SH, North KN *et al.* Mutations in ACTN4, encoding alpha-actinin-4, cause familial focal segmental glomerulosclerosis. *Nat Genet* 2000; 24: 251–256
41. Dai S, Wang Z, Pan X *et al.* Functional analysis of promoter mutations in the ACTN4 and SYNPO genes in focal segmental glomerulosclerosis. *Nephrol Dial Transplant* 2010; 25: 824–835
42. Kretzler M, Koeppen-Hagemann I, Kriz W. Podocyte damage is a critical step in the development of glomerulosclerosis in the uninephrectomised-desoxycorticosterone hypertensive rat. *Virchows Arch* 1994; 425: 181–193
43. Tanca A, Pagnozzi D, Burrai GP *et al.* Comparability of differential proteomics data generated from paired archival fresh-frozen and formalin-fixed samples by GeLC-MS/MS and spectral counting. *J Proteomics* 2012; 77: 561–576
44. Addis MF, Tanca A, Pagnozzi D *et al.* Generation of high-quality protein extracts from formalin-fixed, paraffin-embedded tissues. *Proteomics* 2009; 9: 3815–3823
45. Zhang Y, Yoshida Y, Xu B *et al.* Comparison of human glomerulus proteomic profiles obtained from low quantities of samples by different mass spectrometry with the comprehensive database. *Proteome Sci* 2011; 9: 47
46. Sethi S, Gamez JD, Vrana JA *et al.* Glomeruli of Dense Deposit Disease contain components of the alternative and terminal complement pathway. *Kidney Int* 2009; 75: 952–960
47. Nakatani S, Wei M, Ishimura E *et al.* Proteome analysis of laser microdissected glomeruli from formalin-fixed paraffin-embedded kidneys of autopsies of diabetic patients: nephronectin is associated with the development of diabetic glomerulosclerosis. *Nephrol Dial Transplant* 2012; 27: 1889–1897
48. D'Agati VD, Kaskel FJ, Falk RJ. Focal segmental glomerulosclerosis. *N Engl J Med* 2011; 365: 2398–2411
49. Nagata M, Kriz W. Glomerular damage after uninephrectomy in young rats. II. Mechanical stress on podocytes as a pathway to sclerosis. *Kidney Int* 1992; 42: 148–160
50. Eng E, Veniant M, Floege J *et al.* Renal proliferative and phenotypic changes in rats with two-kidney, one-clip Goldblatt hypertension. *Am J Hypertens* 1994; 7: 177–185
51. Herrmann A, Tozzo E, Funk J. Semi-automated quantitative image analysis of podocyte desmin immunoreactivity as a sensitive marker for acute glomerular damage in the rat puromycin aminonucleoside nephrosis (PAN) model. *Exp Toxicol Pathol* 2012; 64: 45–49
52. Kakimoto T, Okada K, Hirohashi Y *et al.* Automated image analysis of a glomerular injury marker desmin in SDT rats treated with losartan. *J Endocrinol* 2014; 222: 43–51
53. Marshall CB, Kroffit RD, Blonski MJ *et al.* Role of smooth muscle protein SM22alpha in glomerular epithelial cell injury. *Am J Physiol Renal Physiol* 2011; 300: F1026–F1042
54. Wang X, Sakatsume M, Sakamaki Y *et al.* Quantitative histological analysis of SM22alpha (transgelin) in an adriamycin-induced focal segmental glomerulosclerosis model. *Nephron Exp Nephrol* 2012; 120: e1–e11
55. Daniel C, Ludke A, Wagner A *et al.* Transgelin is a marker of repopulating mesangial cells after injury and promotes their proliferation and migration. *Lab Invest* 2012; 92: 812–826
56. Hunt MC, Alexson SE. The role Acyl-CoA thioesterases play in mediating intracellular lipid metabolism. *Prog Lipid Res* 2002; 41: 99–130

Received for publication: 18.2.2014; Accepted in revised form: 20.7.2014